

# LEGIBILITY NOTICE

A major purpose of the Technical Information Center is to provide the broadest dissemination possible of information contained in DOE's Research and Development Reports to business, industry, the academic community, and federal, state and local governments.

Although a small portion of this report is not reproducible, it is being made available to expedite the availability of information on the research discussed herein.

LA-UR--90-2132

DE90 013157

TITLE A Study of Positrons From Soviet Nuclear Powered Satellites  
as Tracers for Magnetospheric Research

AUTHOR(S) E.W. Hones, Jr.

SUBMITTED TO XXVIII COSPAR Plenary Meeting, The Hague, The Netherlands,  
25 June - 6 July 1990

DISCLAIMER

This report was prepared as an account of work sponsored by an agency of the United States Government. Neither the United States Government nor any agency thereof, nor any of their employees, make any warranty, express or implied, or assumes any legal liability or responsibility for the accuracy, completeness, or usefulness of any information, apparatus, product, or process disclosed, or represents that its use would not infringe privately owned rights. Reference herein to any specific commercial product, process, or service by trade name, trademark, manufacturer, or otherwise does not necessarily constitute or imply its endorsement, recommendation, or favoring by the United States Government or any agency thereof. The views and opinions of authors expressed herein do not necessarily state or reflect those of the United States Government or any agency thereof.

By depositing this article in the journal, the author recognizes that the U.S. Government retains a nonexclusive, royalty-free license to publish or reproduce the published form of this contribution or to allow others to do so for U.S. Government purposes.

The U.S. Government is authorized to reproduce and distribute reprints for government purposes, not withstanding any copyright notation that may appear hereon.

Los Alamos Los Alamos National Laboratory  
Los Alamos, New Mexico 87545

MASTER

**A Study of Positrons from Soviet Nuclear Powered  
Satellites as Tracers for Magnetospheric Research**

E. W. Hones

*Mission Research Corporation, Los Alamos, NM 87544\**

**ABSTRACT**

Two Soviet satellites carrying nuclear reactors operated in circular 790 km orbits (65° inclination) in 1987 and 1988. Positrons generated in the satellites' surfaces by the intense reactor gamma radiation escaped and were trapped for periods of minutes to hours in the geomagnetic field. These positrons have been observed on many occasions by gamma ray sensors on the SMM satellite (in 500 km orbit) which identify the positrons by the 511 keV gamma rays created when they annihilate in the satellite surface. The SMM detector provides a time resolution of 64 milliseconds. It has recorded positron rise-times of less than 0.5 second (corresponding to about 1 positron gyroradius) on many occasions as it encounters the low-L edge of positrons injected by the Soviet satellites as far as half-way around the earth. We are studying the potential of these sharply defined positron shells as magnetospheric tracers and as a means for examining particle diffusion and loss processes.

---

\* Also a Guest Scientist at the Los Alamos National Laboratory

## INTRODUCTION

Soviet satellites powered by nuclear reactors have operated in low earth orbits (260 km altitude, 65° inclination) for about 20 years. Nuclear radiations from these were first detected by the Gamma Ray Spectrometer (GRS) experiment on the Solar Maximum Mission (SMM) satellite in 1980 /1/. Notable among the GRS signatures of these radiations were enhancements of the count rate of the .51 MeV gamma ray channel whose purpose was to study positron annihilation radiation from the galactic center and from other natural sources. It was ascertained that the .51 MeV gamma ray enhancements were caused by annihilation, in the SMM satellite's surface, of positrons emitted by the Soviet satellites and trapped in the geomagnetic field /2, 3/.

In February 1987 and again in July 1987 the Soviets placed reactor powered satellites in higher orbits (790 km altitude, 65° inclination). Positrons injected at this higher altitude had a greater chance to escape scattering and loss in the atmosphere so both the intensity and frequency of occurrence of "positron events" recorded by SMM increased to new higher levels (see Figure 4 of /1/).

## OBSERVATIONS AND INTERPRETATION

Figure 1 shows positron encounters by SMM during eleven orbits of the earth or several days in April 1987. Many more encounters were recorded during this period but for the purpose of this report we have selected only some of the most intense events displaying the sharp drops and/or rises seen here. The time resolution of the GRS is 64 milliseconds and close inspection of the data shows that the duration of each sharp drop and rise is typically less than 0.5 sec. SMM was in a near-circular orbit (altitude 480 km, inclination 28 degrees).

Figure 2 depicts schematically the orbits of Cosmos 1818 (the Soviet satellite that was operating during this period in April 1987) and of SMM in the eccentric dipole magnetic field of the earth. Also shown are geomagnetic L-shells in the range 1.00 to 1.20  $R_E$ . As Cosmos 1818 crosses the magnetic equator, it reaches some minimum L value between  $\sim 1.05$  and  $\sim 1.20$  (depending upon its longitude) and skims along that L shell for some time. It is estimated that the positron spectrum emanating from the Soviet satellite decreases monotonically from an intensity of  $\sim 10^{12}$

positrons/MeV/sec at a kinetic energy of a few tenths of an MeV to  $\sim 10^{10}$  positrons/MeV/sec at 4 MeV (see Figure 3 of /3/). The gyro-diameter of a 1 MeV positron on these low L-shells is  $\sim 0.5$  km, so we consider a "positron shell" to consist of those positrons deposited in a 50 km increment of L, i.e., within  $\Delta L = 50/6371 = .00785$ . Positrons drift westward from the longitude of their deposition with a speed proportional to their kinetic energy and depending on their pitch angle as well. (The westward drift speed of a 1 MeV positron is  $\sim 0.1$  degree per second.)

Positrons drifting westward from their longitude of deposition remain on the L-shell on which they were deposited, thus forming a westward moving shell of positrons that also expands westward due to the velocity dispersion associated with their energy-dependent drift speeds. Positrons are also lost from the expanding shell by scattering collisions with air molecules in the upper atmosphere.

Just before it crosses the equator Cosmos 1818 spends 8.0 seconds in the lowest 0.5 km shell that it reaches. It spends 3.3 seconds before that in the next-lowest such shell and 2.5 seconds in the shell before that. In the 20th shell before the lowest (which it crosses 36 seconds before reaching the equator) it spends only 0.9 second. Thus the time available for depositing positrons is by far the greatest in the few shells near the equatorial crossing. We have used this fact, together with the positron spectrum mentioned above (Figure 3 of /3/), and the energy-dependent drift speeds to calculate the evolution of the positron flux distribution westward from the longitude of an equatorial crossing of Cosmos 1818 (Figure 3). The curves show, for example, that SMM, crossing the Cosmos 1818 minimum L-shell (16 sec) 140 degrees west of the Cosmos 1818 crossing, 30 minutes after that crossing occurred, would encounter a positron flux of  $\sim 10$  positrons/cm<sup>2</sup>-sec. It would see a flux of only  $\sim 0.6$  positrons/cm<sup>2</sup>/sec as it crossed the 1 sec shell about one minute earlier.

The reason for the two-peaked distributions in Figure 1 is now evident. As SMM approaches the equator it enters a region of L-shells recently visited by Cosmos 1818 somewhere to the east. SMM eventually reaches L-shells below the minimum L reached by Cosmos 1818 where no positrons were deposited. On the other side of the equator SMM again reaches L-shells above the Cosmos 1818 minimum and again sees positrons. This explanation is illustrated in Figure 4 for event D of Figure 1, whose occurrence time was about 1230 UT. SMM drops to L values below the Cosmos 1818

minimum value for about five minutes about ten minutes after Cosmos 1818 reached it and about 60 degrees west of where Cosmos 1818 reached it (third panel).

Table 1 lists results of detailed analyses we did of the eleven events in Figure 1. At the left we list the minimum L reached by Cosmos 1818, the time,  $t_m$ , when it was reached and the longitude,  $\phi_m$ , at which it was reached. Next we show the time(s),  $t_c$ , calculated for SMM's crossing(s) of that same L value, and the longitude(s),  $\phi_s$ , of that (those) crossing(s). Next are shown the observed time(s),  $t_o$ , of dropout and recovery of the positron flux at SMM. (These times are accurate to  $\sim 0.5$  second or less). The next-to-last column lists the time differences,  $t_c - t_o$ , between predicted and observed positron dropouts and recoveries. The last column lists the azimuthal drift speed (deg/sec) which is  $(\phi_m - \phi_s)/(t_c - t_m)$ .

We point out, first, the relative uniformity of the azimuthal drift speeds. The values average about 0.1 degree per second, which is the approximate drift speed of 1 MeV positrons. This is consistent with the estimated spectrum /3/. The first drift speed of event E2 is notably high, consistent with the fact that the first peak of that event is small, indicating that there are relatively few positrons of energy  $\sim 4$  MeV in the actual spectrum, again as estimated /3/. Note that the observations described here represent time-of-flight measurements of positron drift speed and thus of their kinetic energy. The positrons sampled by SMM in any positron shell are quite highly monoenergetic but with some spread due to the finite range of pitch angles

We next draw attention to the time differences,  $t_c - t_o$ , and note that some of these are quite small (question marks in Events E2 and F2 denote our inability to determine those drop-out times with the usual  $\sim 0.5$  sec. accuracy because of the low instrument count rates). But four events (C1, C2, D, and E1) show large time differences, far greater than the time resolution of the observations. Note, too, that in each event there is first a negative difference and then a positive difference. A possible explanation of these systematic differences is illustrated in Figure 5. The later observed than predicted time ( $T_o > T_p$ ) of positron dropout implies that at SMM's longitude, the equatorial radius of the minimum L shell reached by Cosmos 1818 (60 degrees farther east) is not as great as the magnetic field model predicts. The earlier observed than predicted time ( $T_o < T_p$ ) of positron recovery implies the same thing. All four of these events (C1, C2, D and E1) suggest the same sense

of difference in the L-shell structure over that region of the earth (magnetic longitude range  $\sim 80^\circ$  to  $\sim 160^\circ$ ). The range of discrepancies of the equatorial radius is  $\sim 8$  to 20 km. Alternatively, these discrepancies could be due to errors in calculating the satellite positions (although errors of this magnitude are very unlikely, this matter is being examined), or the result of azimuthal electric fields (all examples involved positron drifts from  $\sim 1800$  to  $\sim 1300$  magnetic local time).

## CONCLUSIONS

Positrons generated by Soviet nuclear powered satellites that operated in high (790 km) orbit for 17 months in 1987 and 1988, and trapped in the geomagnetic field were detected on many occasions by the .51 MeV gamma ray channel of the GRS experiment on SMM. The shells of trapped positrons have sharp, intense lower edges whose locations are determined by the minimum L value reached by the Soviet satellite as it crosses the geomagnetic equator. SMM (in lower orbit than the Soviet satellites) senses the sharp lower edge of the positron belts as sudden dropouts and sudden recoveries of positron flux. The high time resolution (64 milliseconds) of the SMM measurements allows location of the minimum L shell to high precision at locations as much as 90 degrees or more in longitude west of the longitude of their injection. Thus, discrepancies of the real magnetic field from the IGRF 1985 model used in the calculations are potentially recognizable, as are effects of magnetospheric electric fields, geomagnetic storm perturbations of the magnetic field and various dispersive effects on the drifting positrons. One set of observations suggests that discrepancies in the equatorial radius of L-shells as small as 7 km are easily detectable from the data.

## ACKNOWLEDGMENTS

I am grateful to Maj. R. M. Cotton, Maj. M. P. Halpin, and Mr. R. Morris of the U.S. Air Force Space Command for providing orbital elements for the SMM and Cosmos 1818 satellites as well as a program for their use in calculating satellite locations. G. H. Share and D. C. Messina of the U.S. Naval Research Laboratory have been generous in providing data from the GRS on SMM and in aiding in its interpretation. This research was done under the auspices of the U.S. Department of Energy.

## REFERENCES

1. E. Rieger, W. T. Vestrand, D. J. Forrest, E. L. Chupp, G. Kanbach, and C. Reppin, *Science*, **244**, 441 (1989).
2. G. H. Share, J. D. Kurfess, K. W. Marlow, and D. C. Messina, *Science* **244**, 444 (1989).
3. E. W. Hones and P. R. Higbie, *Science* **244**, 448 (1989).



## FIGURE CAPTIONS

Fig. 1. A series of positron encounters recorded by the .51 MeV gamma ray channel of the GRS on SMM in April 1987. Each trace is a record acquired during one complete orbit. Tic marks are 10 minutes apart. The peak positron intensities rise by factors of 10 to 30 above the instrument background.

Fig. 2. A sketch of L-shells in the eccentric dipole model of the earth's magnetic field. Orbits of Cosmos 1818 (and Cosmos 1867) are shown as well as that of SMM (and another satellite, Ginga).

Fig. 3. Estimated longitudinal distribution of positron flux westward from the longitude of a Cosmos 1818 equatorial crossing. Curves are shown for 10 minutes after the crossing and for 30 minutes after the crossing. In each case the distribution is given for the minimum L shell reached (16 second residence time) and for the L-shell crossed about 1 minute before and after the equatorial crossing (1 sec total residence time).

Fig. 4. The top two panels show logarithmic and linear plots of L for SMM and Cosmos 1818 for three hours on April 24, 1987. The curve that reaches the large values of L (top panel) is for Cosmos 1818. The third panel, DMLONG, is the magnetic longitude (measured eastward) of Cosmos 1818 minus that of SMM. The fourth panel shows the magnetic latitudes of the two satellites. Cosmos 1818 goes to the higher latitudes. The points that make up the curves are one minute apart.

Fig. 5. An interpretation of differences between predicted and observed times of positron dropouts and recoveries.

SMM and COSMOS 1818

APRIL 20-29, 1987

EVENT	1818 MINIMUM L			SMM AT SAME L		OBSERVED Time ( $t_o$ )	$t_c - t_o$ (sec)	$(\phi_m - \phi_s) /$ $(t_c - t_m)$
	L	$t_m$	$\phi_m$	$t_c$	$\phi_s$			
4/20 (A)	1.10618	16:03:55	100	16:07:12	81	16:07:08	+4	.111
4/21 (B)	1.10405	15:34:42	103	15:38:47	77	15:38:49	-2	.144
4/23 (C1)	1.04528	11:14:41	160	11:28:55	111	11:29:42	-47	.058
				11:33:21	122	11:32:44	+37	.035
4/23 (C2)	1.07141	12:55:50	135	13:00:30	82	13:00:46	-16	.177
				13:07:25	98	13:07:06	+19	.056
4/24 (D)	1.06649	12:26:28	138	12:32:59	82	12:33:13	-14	.133
				12:38:29	96	12:38:15	+14	.058
4/25 (E1)	1.06190	11:57:06	142	12:05:42	85	12:06:01	-19	.106
				12:09:18	93	12:09:01	+17	.068
4/25 (E2)	1.09360	13:37:53	118	13:39:30	60	?	?	.483
				13:44:50	72	13:44:48	+2	.128
4/26 (F1)	1.08989	13:08:38	121	13:11:50	60	13:11:49	+1	.339
				13:16:04	72	13:16:03	+1	.117
4/26 (F2)	1.10853	14:48:45	95.8	14:49:13	45.2	?	?	
				14:50:36	49.2	14:50:46	-10	.420
4/27 (G)	1.08567	12:39:22	124	12:44:28	63	12:44:34	-6	.169
				12:46:59	69	12:46:46	+13	.115
4/29 (II)	1.04333	08:18:45		1818 Min L not reached by SMM		08:40:12 08:43:11		

### SMM 1987

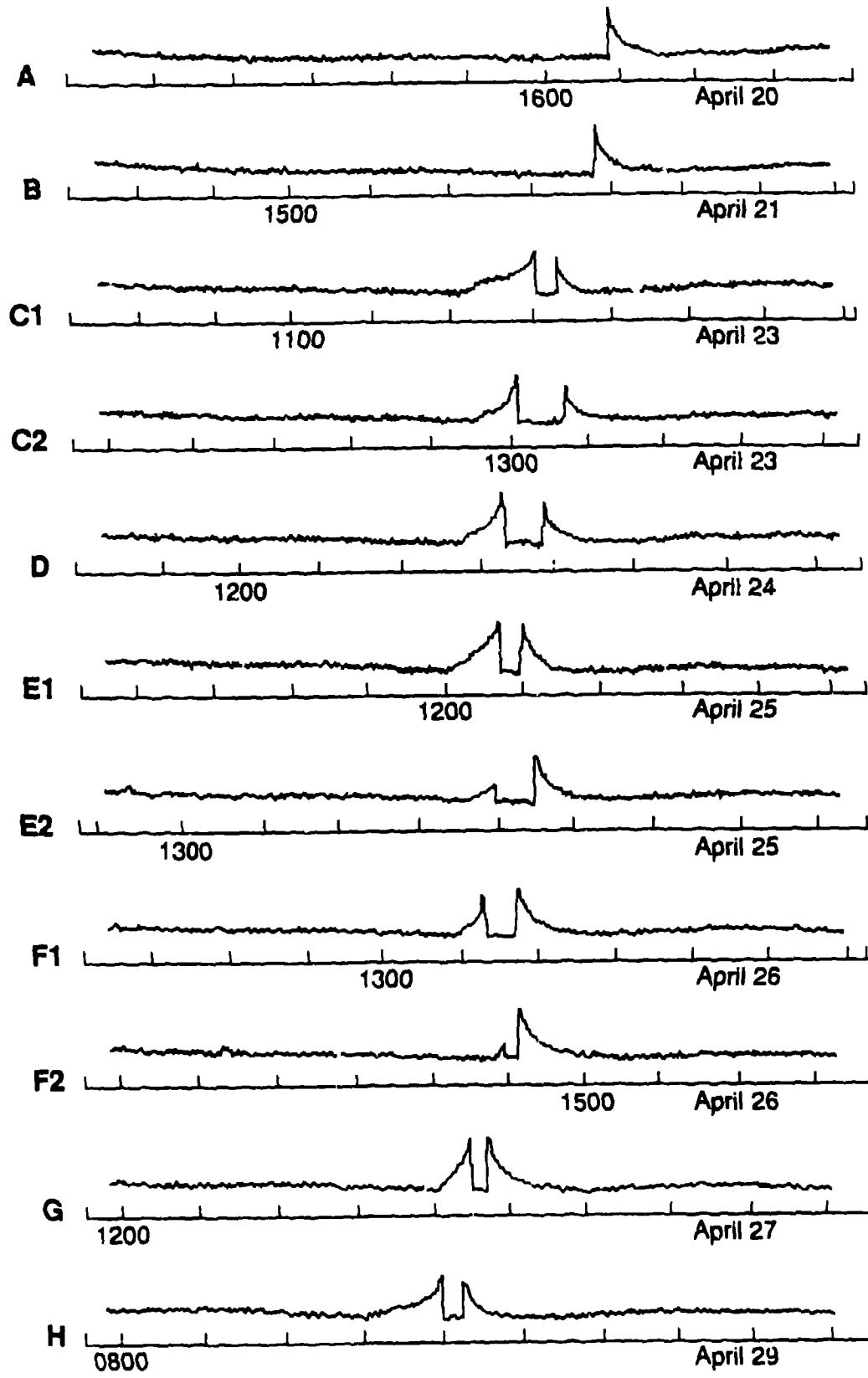


Fig. 1

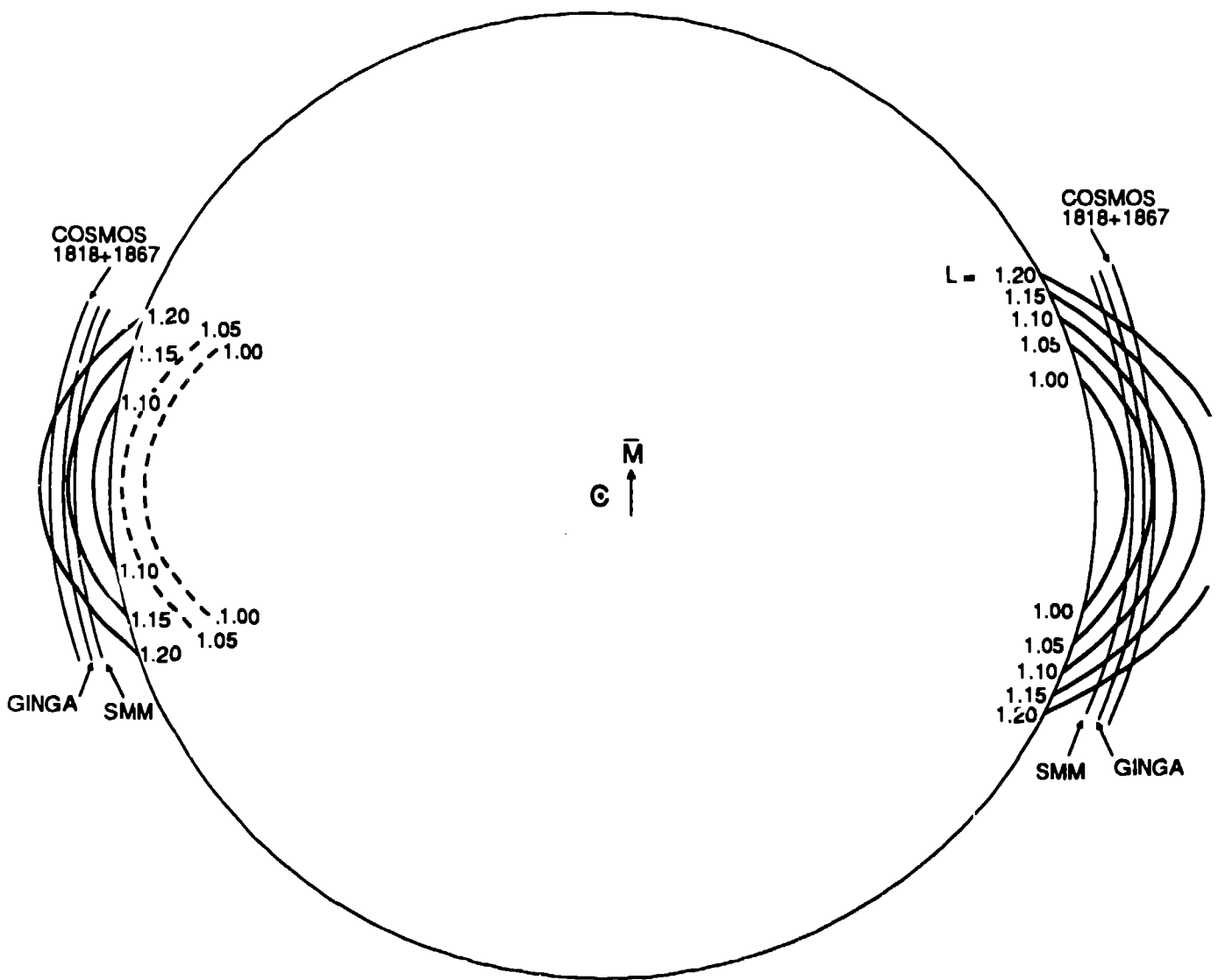


Fig. 2

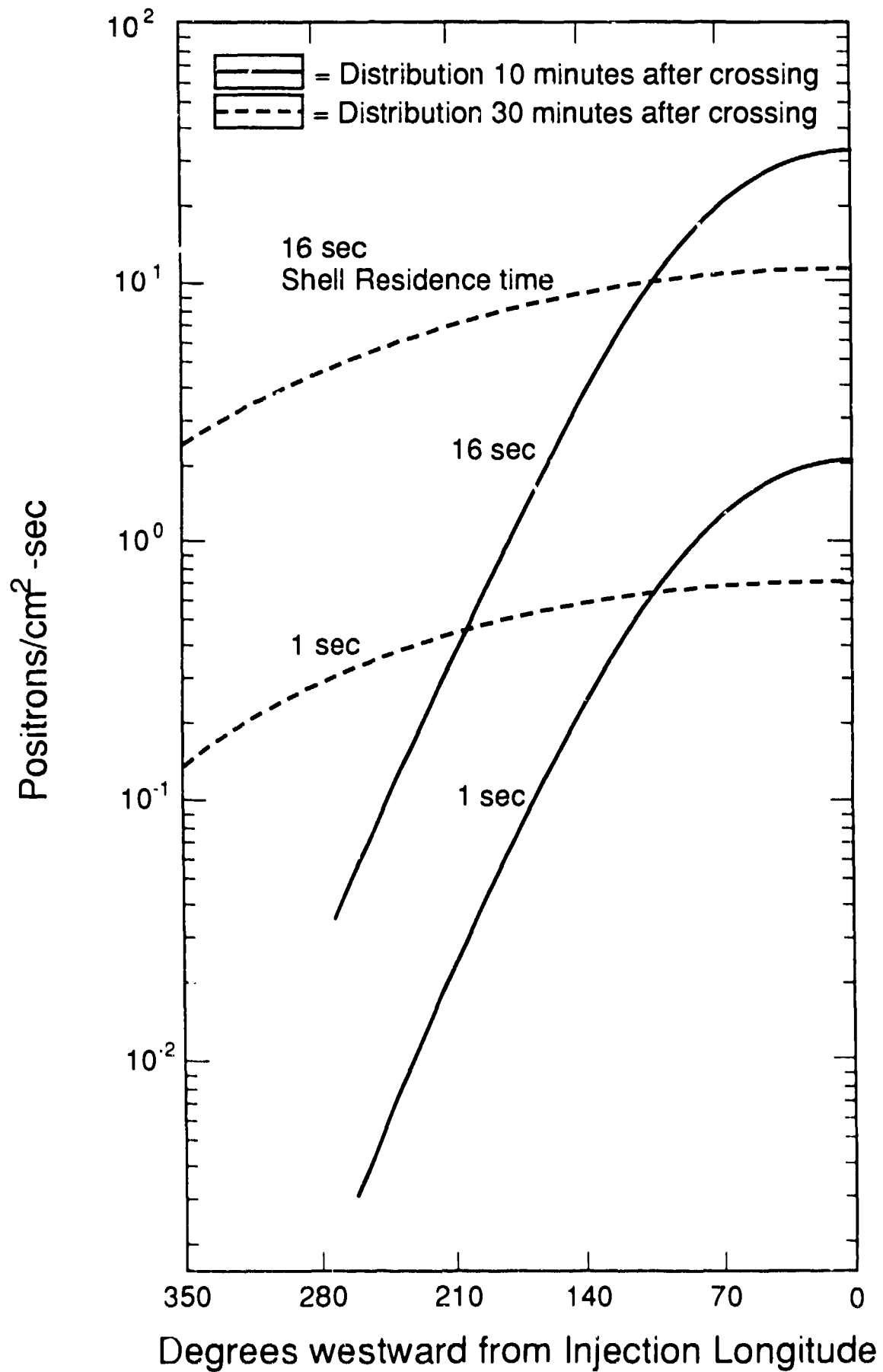


FIG. 3

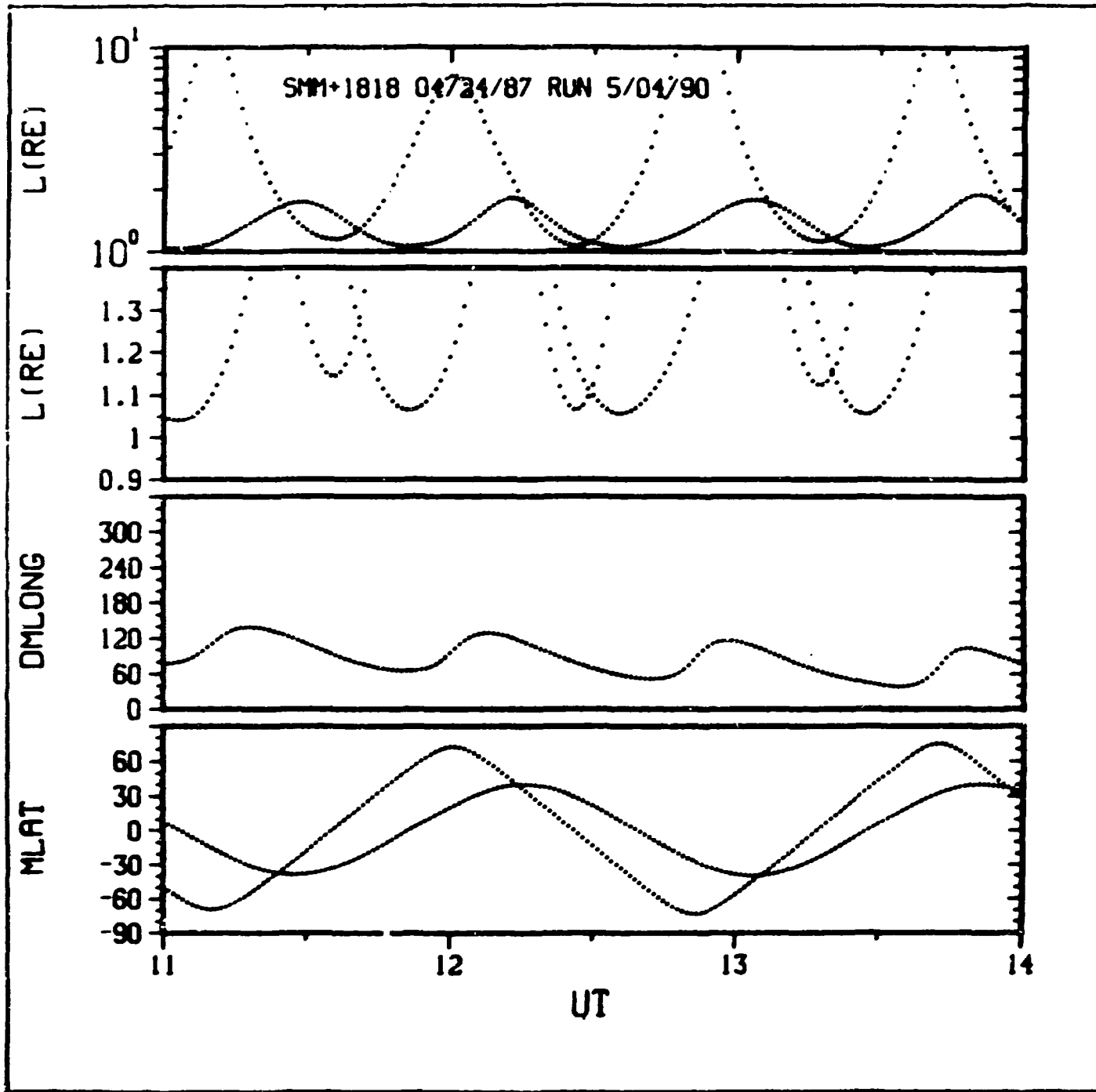


Fig. 4

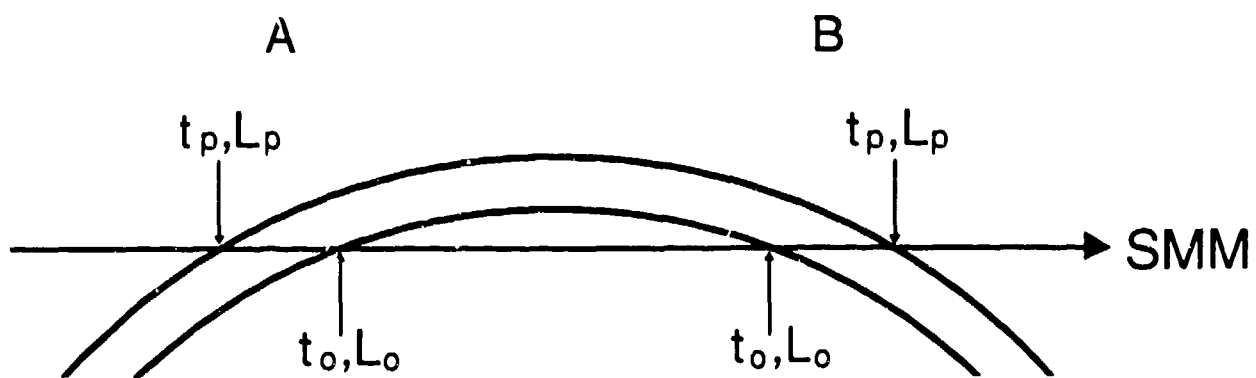


Fig. 5